

M. Y. KHALIL⁽¹⁾, W. A. OMAR⁽²⁾, and K. A. YASSO⁽²⁾

⁽¹⁾*Nuclear Eng. Department, Faculty of Eng., Alex. University*

⁽²⁾*Nuclear Power Plants Authority, P.O. Box 8191, Code No. 11371, Cairo, Egypt*

ABSTRACT

This work is part of an integrated R&D program aiming at developing a computer code that can be used in design review of nuclear fuel and in evaluation of its operational performance in pressurized water reactors. It presents a computer code, Fuel SIMulation (FSIM), which is developed by embedding optimized physical models in a general-purpose finite element computer code (TEPSAC) to predict fuel behavior during normal and operational transients. FSIM is a two-dimensional finite element computational code with axisymmetric (r-z) modeling. It utilizes this technique to calculate the temperature, displacement, stress, and strain distribution in the pellet and sheath. The code can analyze the integral behavior of a whole fuel rod throughout its life, as well as localized behavior of a small part of the fuel rod such as cladding ridge deformation.

To test the code, a sample problem is applied on a generic CANDU-6 reactor, where data of the fuel element and reactor operating conditions have been employed to FSIM. Output results are compared with that produced by ELESIM code and they show a reasonable agreement with that of ELESIM.

1. INTRODUCTION

The work presented here is a part of a comprehensive R & D program aiming at acquiring suitable tools to examine the fuel design and to review safety analysis reports with sufficient and acceptable accuracy. In this area, literature review revealed that there are many computer codes, which are used in evaluating the fuel performance in Pressurized Heavy Water Reactors (PHWRs), for example, ELESIM, ELESTRES, ROFEM, and BACO, as well as FAIR and FUDA. They mostly apply finite difference technique in one dimension to calculate temperature distribution in radial direction to save the computational time, in part, and due to computer capacity limitations, on the one hand. On the other hand, accurate calculation of temperature distribution in the pellet and sheath in two or three dimensions allows better prediction of the physical models such as gas release, fuel expansion and consequently the sheath strains and stresses.

Accordingly, FSIM code has been developed by linking a general-purpose finite element computer code (TEPSAC) with some selected physical models that describe the fuel behavior during irradiation in a semi-mechanistic approach. Basic mathematical structure of FSIM code is presented in section (2), where a summary of the TEPSAC code, is described. In addition, the classical equation for steady state non-linear conduction of heat and the physical models, which are adopted in the thermal analysis, are outlined. Main elastoplastic relations applied in the deformation analysis are also mentioned.

To test the FSIM code capability, a sample problem, as described in Section (3), is applied, where data of fuel elements of a generic CANDU-6 reactor are employed in FSIM and a sample of the output results are compared with output results produced by the fuel performance code, ELESIM. Finally, Section (4) presents the concluding remarks and recommendations for further development.

2. MATHEMATICAL MODELING

2.1 TEPSAC Code

The TEPSAC code performs general thermal and mechanical analyses with the finite element method [1]. The types of analyses solved by TEPSAC are steady state or transient thermal analyses, elastoplastic and creep analyses or any other combination of those. The code uses the Von-Mises formulation to define the yield surface and the Parndtl-Reuss flow rule to define the incremental plastic strains. It can analyze more than one material with different physical properties. The mechanical properties of the materials (Young's modulus, Poisson's coefficient, and plastic modulus, yielding stress) can be expressed as functions of temperature and strain rate.

2.2 FSIM Code

2.2.1 Thermal Analysis

Heat Transfer Models

The fuel pellet and sheath are divided into a finite number of ring elements of quadrilateral cross-section and, moreover, each ring element is subdivided into two ring elements of triangular cross-section. The temperature distribution in the pellet and sheath is calculated at each time step and each mesh point by solving Fourier Equation;

$$\frac{\partial \left(k_{ij} T_{,j} \right)}{\partial r_i} + Q = 0$$

Where, T is the temperature, k_{ij} is the thermal conductivity tensor, Q is the volumetric

heat source, $T_{,j} = \frac{\partial T}{\partial r_j}$. The solution is based on an iterative procedure and

considering the power depression effect in the fuel pellet.

Physical Models

Thermal conductivity of UO_2 can be given by either of two models; SIMFUEL model [2], which is expressed as a function of temperature, porosity, and burnup, and the other one which is given in MATPRO - 9 [3]. The heat transfer coefficient between fuel pellet and sheath is calculated by the modified Ross and Stoute model [4]. The model proposed by Notely and Hastings [5] has been adopted to simulate the gas release, fuel swelling and densification.

2.3.2 Deformation Analysis

Elastoplastic Relations

Elastic behavior of materials can be treated by the linear elastic theory. The constitutive equation is

$$\{\sigma\} = [C_e] \{\varepsilon_e\}$$

where, $\{\sigma\}$ is the stress vector, $[C_e]$ is the elasticity matrix, and $\{\varepsilon_e\}$ is the strain vector.

Materials show elastoplastic deformation when stresses satisfy the following Von Mises yield criterion:

$$F = \sqrt{0.5 \left[(\sigma_r - \sigma_z)^2 + (\sigma_z - \sigma_\theta)^2 + (\sigma_\theta - \sigma_r)^2 + 6\tau_{rz}^2 \right]} - \sigma_y$$

where, $\sigma_r, \sigma_z, \sigma_\theta$ and τ_{rz} are normal and shear stress components in cylindrical coordinates, respectively, and σ_y is uniaxial yield stress. The constitutive equation for the thermoelastic-plastic deformation is:

$$\begin{aligned} \{\sigma\} = & [C_{ep}] \{d\varepsilon\} - [C_{ep}] \left[\{\alpha\} dT + \frac{\partial [C_e]^{-1}}{\partial T} \{\sigma\} dT + \frac{\partial [C_e]^{-1}}{\partial \varepsilon} \{\sigma\} d\varepsilon \right] - \frac{[C_e] \{\sigma'\}}{s} \left[\frac{\partial F}{\partial T} dT \right] \\ & + \frac{\partial F}{\partial \varepsilon} d\varepsilon \end{aligned}$$

where, $\{d\varepsilon\}$ is an incremental strain component vector, $\{\alpha\}$ is the thermal expansion vector, dT is temperature increment, $\{\sigma'\}$ is the deviatoric stress vector, and $[C_{ep}]$, the elastoplasticity matrix, which equals:

$$[C_{ep}] = [C^e] - [C_p]$$

Where,

$$[C_p] = \frac{1}{s} [C_e] \left\{ \frac{\partial F}{\partial \sigma} \right\} \left\{ \frac{\partial F}{\partial \sigma} \right\}^T [C_e]$$

and,

$$s = \left\{ \frac{\partial F}{\partial \sigma} \right\}^T [C_e] \left\{ \frac{\partial F}{\partial \sigma} \right\} - \frac{\partial F}{\partial K} \left\{ \frac{\partial K}{\partial \varepsilon_p} \right\}^T \left\{ \frac{\partial F}{\partial \sigma} \right\}$$

Where, K is a work hardening parameter of material, and $\{d\varepsilon_p\}$ is incremental plastic strain component. These equations are used for deriving the finite element stiffness matrix as followed in [1].

Material Properties

All fuel material properties; thermal expansion, yield strength, Young's modulus, and Poisson's ratio of UO_2 and Zr-4 are as given in MATPRO-9 [3].

3. CODE VALIDATION

In this section FSIM output results are compared with that of ELESIM code for the thermal analysis, and with simple analytical models for deformation analysis. Regarding validation of thermal analysis, although many of the physical processes are represented in FSIM by the same models as in ELESIM, there are many differences between the two codes. The major differences are:

- ◆ FSIM performs the thermal and mechanical analysis using two-dimension axisymmetric finite element technique. This provides FSIM with better capabilities in assessment of stresses and strains in both the fuel and sheath during pellet-clad mechanical interaction.
- ◆ Some models are new in FSIM, e.g. UO_2 thermal conductivity, neutron flux depression, and method of calculating internal voidages of fuel element.

For the purpose of comparisons, as-fabricated fuel rod parameters, reactor operating conditions, and power history pertained to CANDU-6 type are employed to FSIM and ELESIM. In this regard, the following areas were examined:

- ◆ Temperature profile in the pellet at beginning of life (BOL).
- ◆ Influence of power ratings on the fuel temperature.
- ◆ Influence of the as-fabricated density on the fuel temperature.
- ◆ Influence of the power rating on the internal gas pressure.
- ◆ Influence of grain size on fission gas release and fuel temperature.

With respect of validation of deformation analysis, FSIM has been validated against simple analytical models and proved reasonable accuracy. The predicted radial and tangential stress components in the pellet and sheath are presented and figured.

3.1 Input Data

Table 1 illustrates input data of a sample case, relevant to the fuel element of the reference reactor of CANDU type. It includes the various parameters describing the fuel element, and reactor operating conditions. Figure 1 shows a schematic geometry of UO_2 pellet and Zr-4 sheath for which, temperature, strain and stresses calculations are made. It also expresses the terms and definitions used in this paper.

3.2 Output Results

Many of computer runs were made to evaluate the FSIM capabilities in predicting thermal and deformation behavior of CANDU fuel. Results of these runs are figured and presented.

3.1.1 Thermal Analysis

Results of calculations of FSIM code and outcome of the comparison process with ELESIM code for the above mentioned points are figured and discussed in case by case basis.

Temperature profile in the pellet at BOL

Figure 2 shows the temperature distribution in the pellet calculated by FSIM and ELESIM. The temperature is normally highest at the center (~ 2150 °k) and lowest near the pellet clad interface (~ 645 °k). It is remarkable that the two codes produce very close output results.

Influence of power ratings on the fuel temperature

The effect of operating power ratings on the fuel temperature is indicated in Figure 3, where the centerline temperature calculated by FSIM and ELESIM increases as the linear power increases. The figure also shows the good agreement between the two output results. However, FSIM predictions of the centerline temperature during the time of operation tend to be higher than that calculated by ELESIM. Figure 4 shows that as time proceeds, the difference between the two estimates increases and reaches about 120 °k by the end of life (EOL). When comparing this value with a temperature level of (2000 °k), it represents about 6%. This discrepancy is due to using a different method to model the variation of flux depression with time.

Influence of the as-fabricated density on the fuel temperature at BOL

The effect of fuel density on fuel temperature comes through that as density decreases, the effective fuel thermal conductivity decreases and fuel temperature rises. Figure 5 shows the variation of the centerline fuel temperature, as calculated by FSIM, with the changing of fuel density from 92 % to 95%, and 97% of theoretical density (TD), and how far it agrees with that trend. These data have also been compared with that calculated by ELESIM and the results of comparison of (95%TD) is illustrated in Figure 6. As shown, the output result calculated by FSIM is in good agreement with that estimated by ELESIM.

Influence of the power rating on the internal gas pressure

Figure 7 shows the strong reaction between the operating power ratings of the fuel during the irradiation lifetime and the internal gas pressure as predicted by FSIM. It can be noticed that increasing the linear power by 20% (from 50 to 60 kW/m) will significantly increase the internal gas pressure from 4 to 13 MPa (~ 3 times) by the end of life (EOL). This observation agrees with the major CANDU operation trends, and proves the importance of internal gas pressure as a limiting factor of the fuel performance.

In order to examine the accuracy of FSIM predictions, internal gas pressure calculated by the code is benchmarked against that calculated by ELESIM for three power ratings; 30, 50, and 60 kW/m. Figure 8 shows the variation of internal gas pressure with burnup at a power rating of 50 kW/m. From the figure, one can notice that at the BOL, and up to 140 MWh/kg U, pressure calculated by FSIM (0.646 MPa) is lower than that calculated by ELESIM (0.849 MPa). After that, FSIM predictions become higher (4.73 MPa) than that calculated by ELESIM (4.1 MPa) at the EOL. This behavior is due to the impact of gradual degradation of heat transfer coefficient of pellet - sheath gap that leads to increasing the fuel temperature. As indicated in Figure 4, fuel temperature calculated by FSIM tends to be

higher than that calculated by ELESIM, and the direct effect of that is more fission gas released and higher pressure estimated by FSIM.

Influence of grain size on fission gas release

Experimental results indicate that initial grain size strongly affects the fission gas release and reduces fractional release with increasing it. This is due to the increase of the diffusion length with large grains. FSIM predictions of the effect of initial grain size are illustrated in Figure 9 for grain sizes of 7.5, 20, and 50 μm . To verify that FSIM provides reasonable output results, gas pressure calculated by FSIM is compared with that produced by ELESIM for grain sizes of 7.5 μm . Figure 10 shows the variation of gas pressure calculated, by FSIM and ELESIM, with burnup for grain size of 7.5 μm . It can be noticed that gas pressure calculated by FSIM tends to be low relative to that predicted with ELESIM. The discrepancy in gas pressure reaches about 4.6 % at EOL. Although the volume of gas released calculated by FSIM is higher than that estimated by ELESIM, the internal voidage calculated by FSIM is higher, which results in lower pressure. This is due to the different ways used in FSIM to calculate the volume of pellet dishes, cracks, and air gaps tends to be lower compared with that calculated by ELESIM.

3.1.2 Deformation Analysis

To test FSIM in predicting of fuel rod deformation, under thermal and mechanical loads, two cases with different operating conditions are considered. The first is to calculate stresses in the pellet and sheath when a gap exists between them. The second case is to calculate stresses when there is a hard contact between pellet and sheath.

Case (1): Gap is open

Figure 11 shows the stress distribution in the pellet and sheath at low power, 30 kW/m, and at BOL. This is to avoid high thermal expansion of the pellet and the swelling effects in closing the pellet-sheath gap. Therefore, the only applied loads are the coolant pressure, which acts on the outer sheath surface and inside gas pressure, which acts on the inner sheath surface and pellet outer surface. It is assumed that both pellet and sheath are placed between rigid end supports, i.e. plane strain assumption exists.

In this case, both pellet and sheath are treated as two separate components. Stresses in the pellet are due to thermal load of temperature gradient along the pellet radius and inner gas pressure as mechanical load. As shown in Figure 11, radial stress equals tangential stress of 290 MPa at the pellet center. It is also noted that radial stress equals 0.495 MPa at the pellet surface and tangential stress changed from compression in the inner zones of the pellet to tension at outer zones. This is due to the high temperature gradient within the UO_2 , which leads to different degrees of expansion and finally causes fuel to crack.

Regarding stress distribution in the sheath, as illustrated in Figure 11, radial stress equals gas pressure (0.495 MPa) at sheath inner surface and increases along the sheath radius up to 10.65 MPa, coolant pressure, at the sheath outer radius. Tangential stress tends to be compressive because coolant pressure is higher than inner gas pressure and varies from 178 MPa. at inner surface to 139 MPa at the outer radius. Stresses in the gap elements vanish to zero, where gap elements are modeled to behave as a compressible fluid.

Case (2): Gap is closed

Figure 12 shows the stress distribution in the pellet and sheath at relatively higher power, 60 kW/m. This leads to gap closure due to thermal expansion of the pellet as well as sheath collapse under the mechanical loads exerted by coolant pressure. In contrast to the previous case, both pellet and sheath are treated as one component and all the gap elements have been modeled to behave as incompressible fluid to transmit stresses introduced in the pellet to the sheath and vice versa.

Accordingly, stress distribution in the pellet is similar to that described in the above case but is different in magnitude, where the compressive radial stress equals 840 MPa at the pellet center and decreases to 87.7 MPa, the interfacial pressure, at pellet-sheath interface. Tangential stress which tends to be compressive in the inner zones equals radial stress at the pellet center, and turns to become tension at radius of 3.9 mm then reaches maximum value of 1000 MPa at outer pellet radius.

Regarding stress distribution in the sheath, radial compressive stress equals the interfacial pressure, 87 MPa, at the pellet- sheath interface, and 10.65 MPa at sheath outer surface. Tangential stress, in this case, tends to tension due to pellet expansion which, makes sheath expand outward. It equals 480 MPa at the sheath inner radius, and decreases along its thickness to be 450 MPa at the outer surface.

4. CONCLUSION

A computer code FSIM has been developed to analyze the thermal and mechanical behavior of heavy water fuel rod during its irradiation life. The cases applied to FSIM code show that there is a good agreement between the results and the CANDU fuel behavior database. However, efforts should be made to improve the accuracy of the solution such as exact treatment of pellet-sheath contact problem and better modeling of flux depression to account for the effect plutonium build up on pellet temperature distribution throughout fuel burnup. It is expected that FSIM code can be used as a tool to study the thermal and mechanical behavior of heavy water fuel rods and as a tool to review the fuel rod design.

5. ACKNOWLEDGEMENTS

The authors would like to thank Dr. S. B. Abdel Hamid, executive chairman of the Nuclear Power Plants Authority for his encouragement and support. They are also so grateful to Dr. Y. M. Ibrahiem and Eng. M. A. El- Sharaky for their cooperation. Special thanks are due to Dr. I. A. El Osery for his continuous assistance.

6. REFERENCES

1. HSU, T. R., "The Finite Element Method in Thermomechanics," Allen & Unwin, Boston, (1986).
2. LUCUTA, P. G., et al. Journal of Nuclear Materials, 188, p. 198-204, (1992)
3. MATPRO-09, " A Handbook of Materials properties for Use in the Analysis of Light Water Reactor Fuel Behavior", TREE-NUREG-1005, (1976).
4. ROSS, A. M., et al., "Heat Transfer Coefficient Between UO₂ and Zircaloy-2," AECL-1552, (1962).

5. CAMBELL, F. R., et al., "In-Reactor Measurement of Fuel to Sheath Heat Transfer Coefficients Between UO_2 and Stainless Steel", AECL-5400, 1974.
6. NOTLEY, M. J. F., et al., "A Microstructure Dependent Model for Fission Product Gas Release and Swelling in UO_2 Fuel", AECL-5838, (1978).

TABLE 1: INPUT DATA OF THE SAMPLE CASE

Parameter	Unit	Value	Remarks
1-Pellet Data			
-Number of pellets in the fuel rod	-	60	
-Pellet diameter	m	12.15 E-3	
-Diameter of central hole	m	0.0	
- UO_2 density	Fraction	0.95	
-Coeff. of thermal expansion	$\mu\text{m}/\text{m.k}$	-	As per MATPRO - 9
-Length of fuel stack	m	0.480	
- UO_2 grain size	μm	7.5	
2- Element Data			
-Diameter clearance	m	0.084E-3	
-Sheath wall thickness	m	0.42E-3	
-Volume of filling gas	mm^3	8790	
-Volume of He fraction	Fraction	0.8	
3- Clad Data			
-Thermal conductivity	$\text{kW} / \text{m} . \text{k}$	-	As per MATPRO-9
-Coeff. of thermal expansion	$\mu\text{m} / \text{m} . \text{k}$	-	As per MATPRO -9
4- Heat Transfer Data			
-Film heat transfer coeff.	$\text{kW} / \text{m}^2 . \text{k}$	40.74	As in ELESIM Manual
-Sheath surface roughness	μm	0.5	
-Fuel surface roughness	μm	0.1	
5- Operational Parameters			
-Enrichment	Percent	0.711	
-Coolant temperature	$^{\circ}\text{k}$	550.0	As in ELESIM Manual
-Coolant pressure	MP_a	10.65	As in ELESIM Manual
-Power history(power / burnup)	$(\text{kW} . \text{m}^{-1} / \text{MWh} . \text{kg}^{-1} \text{U})$	58.1 / 10.0 58.3 / 20.0 58.6 / 30.0 58.8 / 40.0 58.9 / 50.0 59.0 / 60.0 59.1 / 70.0 59.1 / 80.0 58.9 / 90.0 58.6 / 100.0 58.2 / 110.0 57.7 / 120.0 57.1 / 130.0 56.3 / 140.0 55.4 / 150.0 54.4 / 160.0 53.3 / 170.0 52.1 / 180.0 51.1 / 190.0 50.2 / 200.0	

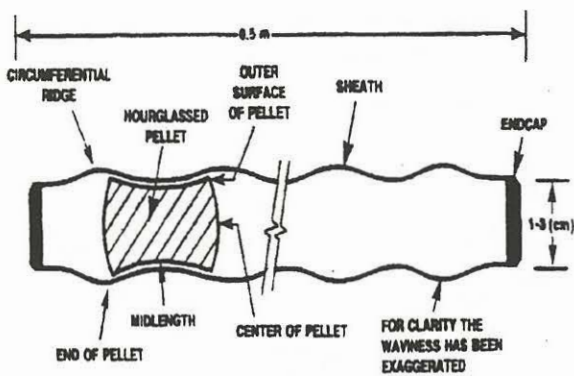


FIGURE 1: FUEL ELEMENT

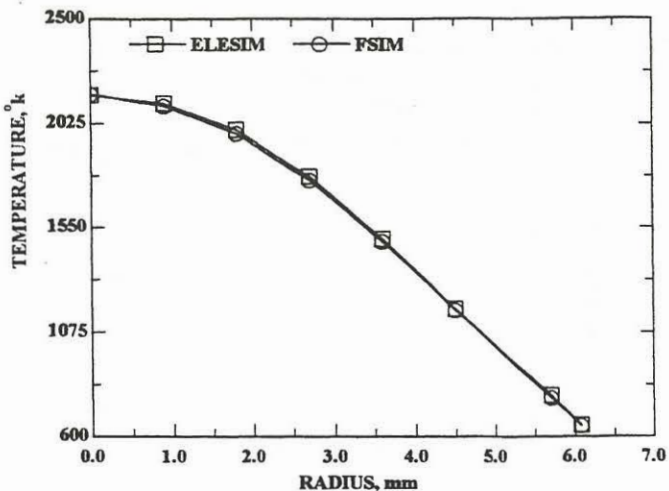


FIGURE 2: COMPARISON OF FSIM AND ELESIM CALCULATIONS OF TEMPERATURE ACROSS THE PELLETS RADIUS

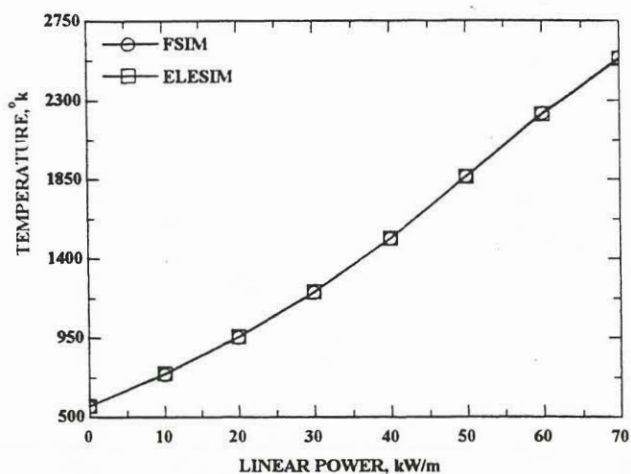


FIGURE 3: COMPARISON OF FSIM WITH ELESIM CALCULATIONS OF CENTERLINE TEMPERATURE AT DIFFERENT POWER RATINGS

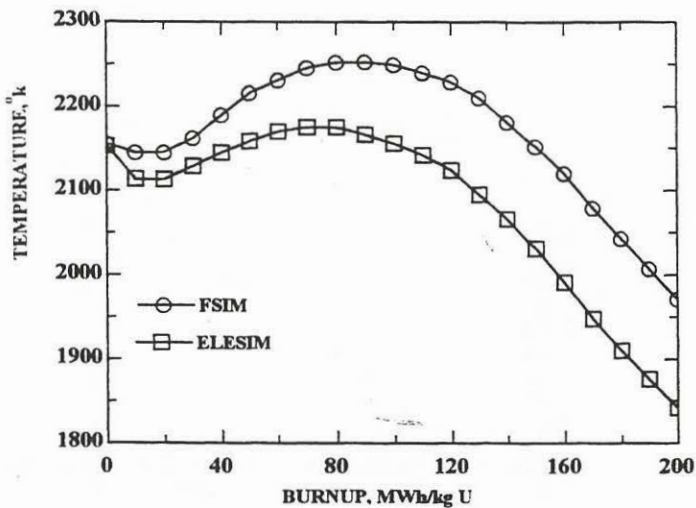


FIGURE 4: COMPARISON OF FSIM WITH ELESIM CALCULATIONS OF PELLETS CENTERLINE TEMPERATURE

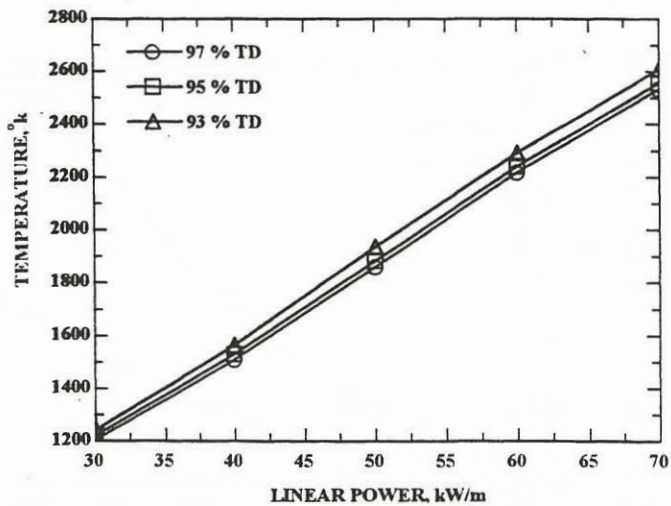


FIGURE 5: FSIM CALCULATIONS OF CENTERLINE TEMPERATURE AT DIFFERENT FUEL DENSITIES

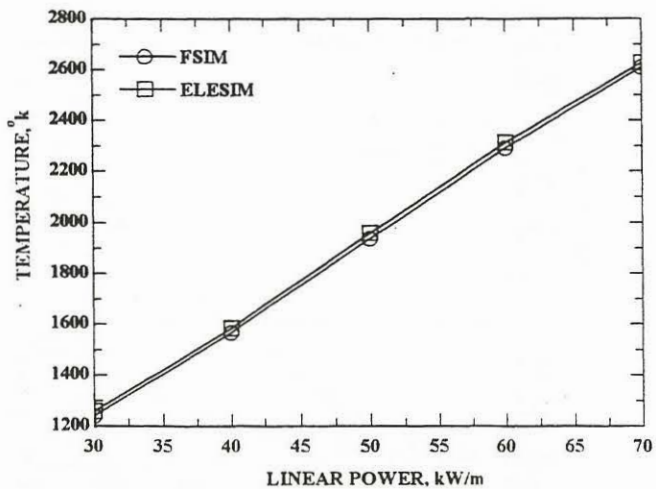


FIGURE 6: COMPARISON OF FSIM WITH ELESIM CALCULATIONS OF CENTERLINE TEMPERATURE (95% THEORETICAL DENSITY)

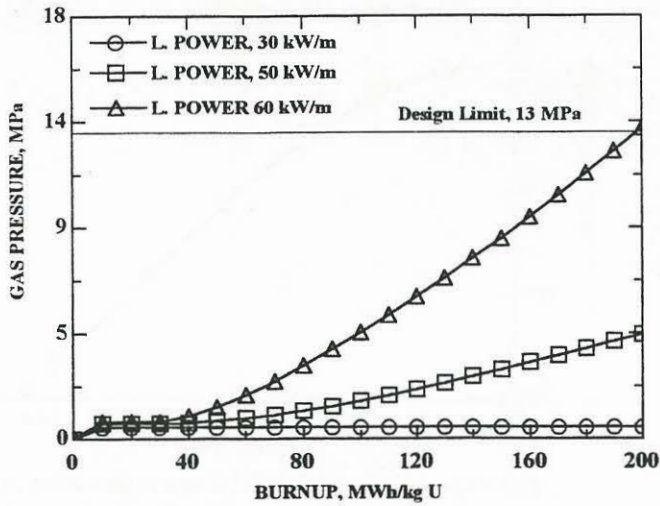


FIGURE 7: FSIM CALCULATIONS OF INTERNAL GAS PRESSURE AT DIFFERENT POWER RATINGS

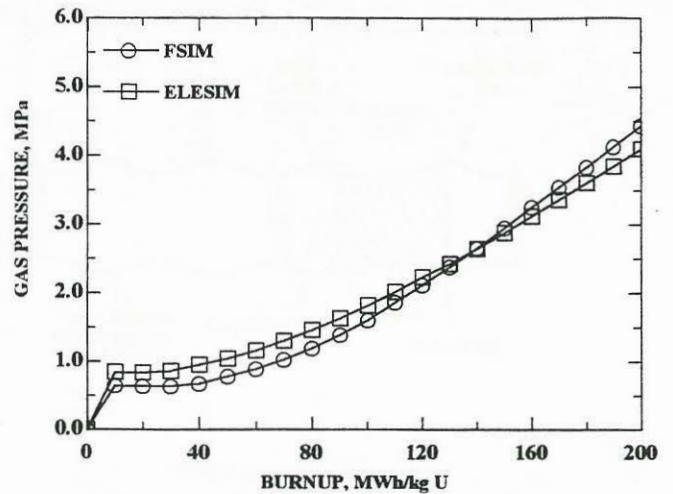


FIGURE 8: COMPARISON OF FSIM WITH ELESIM CALCULATIONS OF INTERNAL GAS PRESSURE (LINEAR POWER = 50 kW/m)

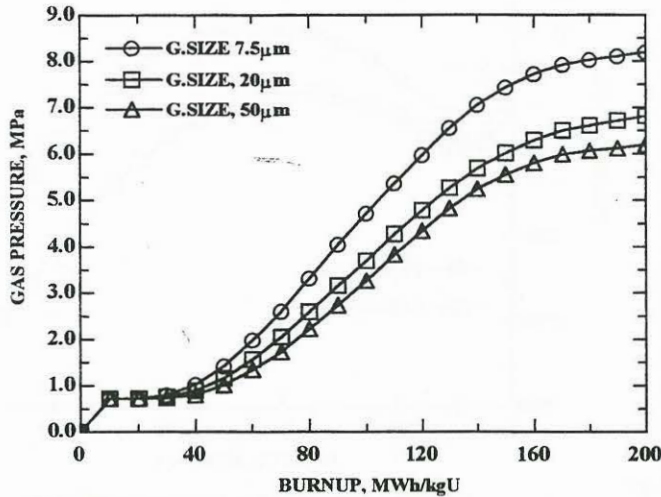


FIGURE 9: FSIM CALCULATIONS OF INTERNAL GAS PRESSURE AT DIFFERENT GRAIN SIZES

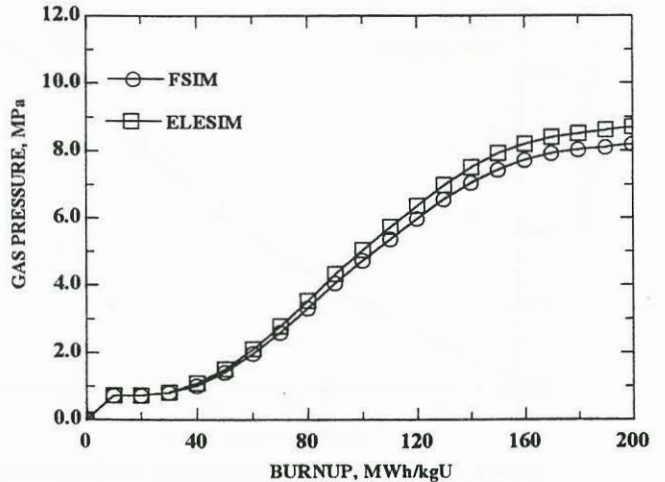


FIGURE 10: COMPARISON OF FSIM WITH ELESIM CALCULATIONS OF INTERNAL GAS PRESSURE - GRAIN SIZE = 7.5 μm

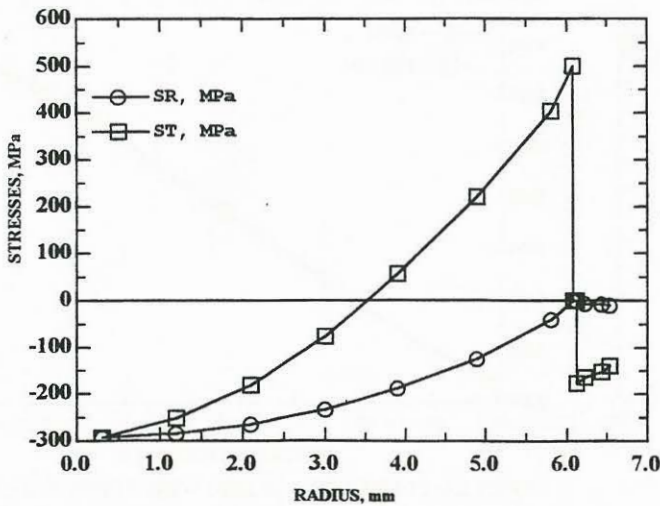


FIGURE 11: FSIM CALCULATIONS OF FUEL ROD RADIAL AND TANGENTIAL STRESSES AT POWER = 30 kW/m

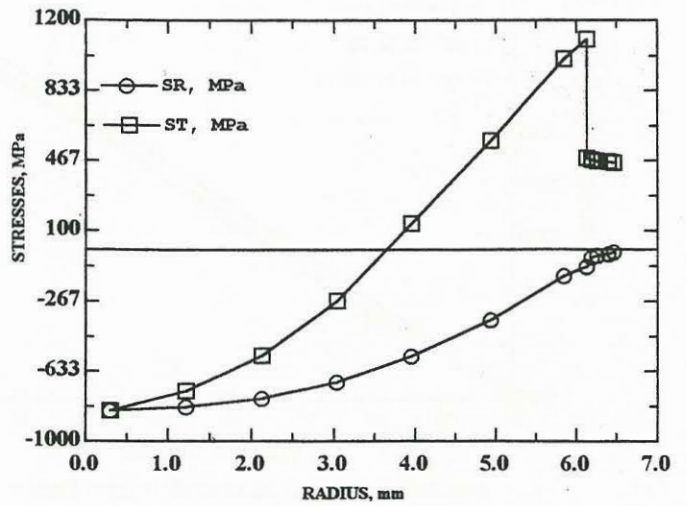


FIGURE 12: FSIM CALCULATIONS OF FUEL ROD RADIAL AND TANGENTIAL STRESSES AT POWER 60 kW/m